Inorganic Chemistry

Article

pubs.acs.org/IC

Dicarboxylate Recognition Properties of a Dinuclear Copper(II) Cryptate

Pedro Mateus,*[,†] Rita Delgado,*[,†] Vânia André,[‡] and M. Teresa Duarte[‡]

[†]Instituto de Tecnologia Química e Biológica António Xavier, Universidade Nova de Lisboa, Avenida da República, 2780-157 Oeiras, Portugal

[‡]Centro de Química Estrutural, Instituto Superior Técnico, Universidade de Lisboa, Avenida Rovisco Pais, 1049-001 Lisboa, Portugal

Supporting Information

ABSTRACT: A ditopic polyamine macrobicyclic compound with biphenylmethane spacers was prepared, and its dinuclear copper(II) complex was studied as a receptor for the recognition of dicarboxylate anions of varying chain length in H_2O/MeOH (50:50 (v/v)) solution. The acid−base behavior of the compound, the stability constants of its complexes with Cu^{2+} ion, and the association constants of the copper(II) cryptate with succinate (suc^{2-}), glutarate (glu^{2-}), adipate (adi^{2-}), and pimelate (pim^{2-}) were determined by potentiometry at 298.2 ± 0.1 K in H_2O/MeOH (50:50 (v/v)) and at ionic strength 0.10 ± 0.01 M in KNO_3. The association constants of the same cryptate as receptor for aromatic dicarboxylate substrates, such as phthalate (ph^{2-}), isophthalate (iph^{2-}), and terephthalate (tph^{2-}), were determined through competition experiments by spectrophotometry in the UV region. Remarkably high values of association constants in the range of 7.34−10.01 log units were found that are, to the best of our knowledge, the highest values of association constants reported for the binding of dicarboxylate anions in aqueous solution. A very well defined peak of selectivity was observed with the binding constant values increasing with the chain length and reaching the maximum for substrates with four carbon atoms between the carboxylate groups. Single-crystal X-ray diffraction determinations of the cascade complexes with adi^{2-} and tph^{2-} assisted in the understanding of the selectivity of the cryptate toward these substrates. The Hirshfeld surface analyses of both cascade complexes suggest that the establishment of several van der Waals interactions between the substrates and the walls of the receptor also contributes to the stability of the associations.

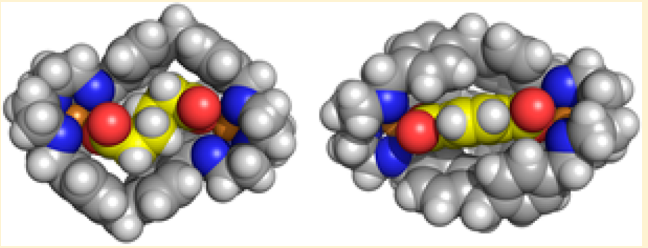

INTRODUCTION

For over 30 years supramolecular chemists have strived to design new synthetic receptors for the recognition of dicarboxylates, owing to the biological and environmental importance of this class of anionic substrates.[1] Indeed, they are key metabolites in the Krebs cycle and their analysis in biological fluids can provide useful information for diagnosis of metabolic disorders and neurological diseases.[2] Monitoring their presence in the environment is also important as they are abundant in atmospheric aerosols and can act as cloud condensation nuclei and, eventually, influence Earth's radiative forcing and climate.[3] Clearly the recognition of this class of substrates is of great biological, medicinal, and environmental relevance, and the design of selective artificial receptors may lead to new or improved methodologies for faster and simpler chemical analysis and detection of these targets.

However, if selective recognition of inorganic anions by artificial receptors in water is already a difficult task, recognition of dicarboxylate anions is even more challenging. Dicarboxylates are highly hydrated anionic species and occur in a wide variety of sizes and conformations. It is thus necessary to develop large receptors with suitable topologies that match a particular size and/or conformation, capable of establishing multiple and strong intermolecular interactions.

Polyamine compounds have been widely used as receptors for the binding of dicarboxylate anions in aqueous medium,[4] because when protonated, the resulting ammonium centers can interact via electrostactic and hydrogen bonding with the anionic substrates and increase the water solubility. Unfortunately, their usefulness as dicarboxylate receptors is limited by the fact that they are only fully protonated in acidic medium while dicarboxylates only exist as dianionic species in a relatively narrow pH window, in general above around pH 7. Alternatively, the formation of cascade species by the selective coordination of a dicarboxylate substrate between the metal centers of a dinuclear complex of a ditopic polyamine macrocycle or cryptand[5] can offer advantages. Among the advantages it is possible to mention the rather high energy of a coordination bond when compared to electrostatic and hydrogen bonding interactions, and consequently higher affinities for the anions; the dinuclear species usually exist at neutral pH, at which the dicarboxylates are dianionic; selectivity

Received: September 12, 2014
Published: December 8, 2014

can be achieved for the dianion with the correct "bite length", that is, the correct distance between the metal centers.[6] Indeed, association constants on the order of 4−8 log units have been determined for the binding of dicarboxylates by dicopper(II) complexes of ditopic polyamine macrocycles and cryptands, which testify to the success of the approach.

Back in the infancy of the field of anion recognition, Lehn et al. reported a polyamine cryptand with a large spacer formed by a biphenylmethane group (L; Chart 1.) capable, when

Chart 1. Cryptand L

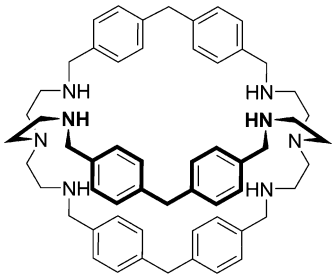

protonated, of encapsulating the terephthalate dianion, as evidenced by the rather beautiful crystal structure.[4f,7] The inclusion of substrates of appropriate size between the metal centers of a dinuclear complex of that cryptand was also envisaged by the authors;[7] however, this work was never performed. Such a study deserves to be undertaken. Therefore, in this work, the acid−base behavior and the copper(II) complexation properties of this polyamine cryptand, L (see Chart 1) were studied for the first time, as well as the recognition of dicarboxylate substrates by its dinuclear copper(II) complex.

RESULTS AND DISCUSSION

Acid−Base Behavior and Copper(II) Coordination Studies. Solution studies were performed by potentiometry to determine the protonation constants of L, as well as the stability constants of its copper(II) complexes. The results, which are crucial for the following studies, are presented in Table 1 (and Tables S1 and S2 in the Supporting Information).

Precipitation of the cryptand occurred at pH 6.0 in aqueous solution; thus, it was necessary to study the compound in mixed solvent H_2O/MeOH (50:50 (v/v)) at T = 298.2 ± 0.1 K and I = 0.10 ± 0.01 M in KNO_3. As expected, six protonation constants were found for L in the working pH region (3.2−11.0), corresponding to the successive protonations of the secondary amines. The corresponding species distribution diagram can be found in Figure S1 in the Supporting Information.

For 2:1 Cu:L ratio, the dinuclear species predominates at a large pH range (from about pH 4; see Figure 1). Even at a 1:1

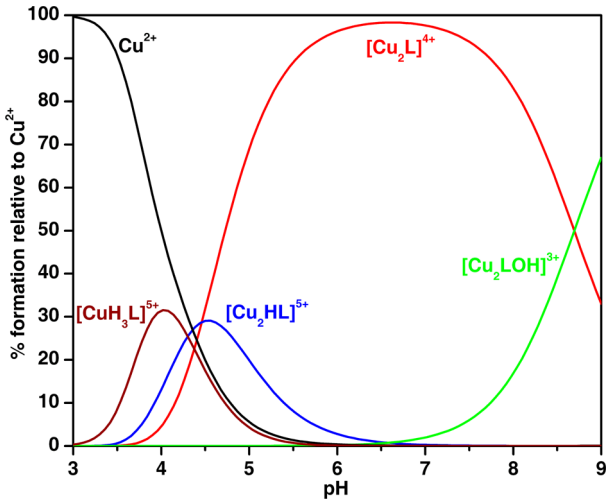

Figure 1. Species distribution diagram calculated for the complexes of Cu^{2+} with L. $C_{Cu} = 2C_L = 2.0 \times 10^{-3}$ M.

Cu:L ratio the dinuclear complexes are also present in significant amounts (Figure S2 in the Supporting Information), confirming the high tendency of this cryptand to coordinate two copper(II) ions. The $[Cu_2L]^{4+}$ species, the most important for the anion binding studies, is rather stable and predominates over a large pH range (4.5−8.5), reaching its maximum percentage at pH 6.6, at which all studied dicarboxylates are generally in the dianionic form (see Table S3 in the Supporting Information).

Cascade Species Formed by the Copper(II) Complexes of L. The association constants of copper(II) complexes of L with the aliphatic dicarboxylate substrates were determined by potentiometry at the experimental conditions used before. The results are collected in Table 2.

Unfortunately, it was not possible to determine the association constants of $[Cu_2L]^{4+}$ with the aromatic dicarboxylate substrates by potentiometry due to precipitation of the supermolecules at low pH. To circumvent this problem, titrations were performed by spectrophotometry in the UV region which allowed the use of much more diluted conditions

Table 1. Equilibrium Constants of the Protonation (K_i^H)[a] of L and Its Complexation ($K_{M_mH_hL_l}$)[a] Equilibria with Copper(II) in H_2O/MeOH (50:50 (v/v))[b,c]

equilibrium reaction	log K_i^H	equilibrium reaction	log $K_{M_mH_hL_l}$
$L + H^+ \rightleftharpoons HL^+$	9.40(1)	$[CuH_2L]^{4+} + H^+ \rightleftharpoons [CuH_3L]^{5+}$	5.54(1)
$HL^+ + H^+ \rightleftharpoons H_2L^{2+}$	9.13(1)	$[CuHL]^{3+} + H^+ \rightleftharpoons [CuH_2L]^{4+}$	7.23(1)
$H_2L^{2+} + H^+ \rightleftharpoons H_3L^{3+}$	7.59(1)	$[CuL]^{2+} + H^+ \rightleftharpoons [CuHL]^{3+}$	8.54(1)
$H_3L^{3+} + H^+ \rightleftharpoons H_4L^{4+}$	7.03(1)	$Cu^{2+} + L \rightleftharpoons [CuL]^{2+}$	14.84(2)
$H_4L^{4+} + H^+ \rightleftharpoons H_5L^{5+}$	5.78(1)	$[CuL(OH)]^+ + H^+ \rightleftharpoons [CuL]^{2+}$	9.84(2)
$H_5L^{5+} + H^+ \rightleftharpoons H_6L^{6+}$	5.66(1)	$[Cu_2L]^{4+} + H^+ \rightleftharpoons [Cu_2HL]^{5+}$	4.46(1)
		$[CuL]^{2+} + Cu^{2+} \rightleftharpoons [Cu_2L]^{4+}$	11.16(1)
		$[Cu_2L(OH)]^{3+} + H^+ \rightleftharpoons [Cu_2L]^{4+}$	8.71(3)

[a]The overall values of all constants are presented in Tables S1 and S2 in the Supporting Information. [b]T = 298.2 ± 0.1 K; I = 0.10 ± 0.01 M in KNO_3. [c]Values in parentheses are standard deviations in the last significant figure.

dx.doi.org/10.1021/ic502230q | Inorg. Chem. 2015, 54, 229−240

Table 2. Overall ($\beta_{Cu_mH_hL_lA_a}$) and Stepwise ($K_{Cu_mH_hL_lA_a}$) Association Constants for the Indicated Equilibria in H_2O/MeOH (50:50 (v/v))[a]

	log $\beta_{Cu_mH_hL_lA_a}$[c]			
equilibrium reaction[b]	suc^{2-}	glu^{2-}	adi^{2-}	pim^{2-}
$2Cu^{2+} + L + A^{2-} \rightleftharpoons [Cu_2L(A)]^{2+}$	33.75(1)	34.50(1)	36.01(1)	33.34(1)
$2Cu^{2+} + L + A^{2-} \rightleftharpoons [Cu_2L(OH)(A)]^{+} + H^{+}$	22.99(2)	23.58(3)	23.97(5)	23.04(2)
$Cu^{2+} + L + A^{2-} \rightleftharpoons [CuL(A)]$	19.49(4)	19.90(5)	20.44(6)	19.27(5)
$Cu^{2+} + H^{+} + L + A^{2-} \rightleftharpoons [CuHL(A)]^{+}$	28.61(4)	28.96(4)	29.61(6)	28.67(4)
$Cu^{2+} + 2H^{+} + L + A^{2-} \rightleftharpoons [CuH_2L(A)]^{2+}$	35.81(3)	36.20(4)	36.77(5)	36.36(2)
$Cu^{2+} + 3H^{+} + L + A^{2-} \rightleftharpoons [CuH_3L(A)]^{3+}$	41.78(3)	42.21(3)	42.91(3)	41.94(2)
$Cu^{2+} + 4H^{+} + L + A^{2-} \rightleftharpoons [CuH_4L(A)]^{4+}$	46.17(1)	45.96(4)		46.19(2)
$Cu^{2+} + L + A^{2-} \rightleftharpoons [CuL(OH)(A)]^{+} + H^{+}$	9.06(5)	9.00(5)		8.99(5)
	log $K_{Cu_mH_hL_lA_a}$			
equilibrium reaction[b]	suc^{2-}	glu^{2-}	adi^{2-}	pim^{2-}
$[Cu_2L]^{4+} + A^{2-} \rightleftharpoons [Cu_2L(A)]^{2+}$	7.75(3)	8.50(1)	10.01(1)	7.34(3)
$[Cu_2L(OH)]^{+} + A^{2-} \rightleftharpoons [Cu_2L(OH)(A)]^{+}$	5.70(4)	6.29(4)	6.68(6)	5.75(9)
$[CuL]^{2+} + A^{2-} \rightleftharpoons [CuL(A)]$	4.65(5)	5.06(5)	5.61(6)	4.43(5)
$[CuHL]^{3+} + A^{2-} \rightleftharpoons [CuHL(A)]^{+}$	5.23(4)	5.58(4)	6.23(6)	5.29(4)
$[CuH_2L]^{4+} + A^{2-} \rightleftharpoons [CuH_2L(A)]^{2+}$	5.20(3)	5.59(4)	6.16(5)	5.75(2)
$[CuH_2L]^{4+} + HA^{-} \rightleftharpoons [CuH_3L(A)]^{3+}$	5.07(3)	5.73(3)	6.40(3)	5.39(2)
$[CuH_3L]^{5+} + HA^{-} \rightleftharpoons [CuH_4L(A)]^{4+}$	3.92(2)	3.94(4)		4.09(2)
$[CuL(OH)]^{+} + A^{2-} \rightleftharpoons [CuL(OH)(A)]^{-}$	4.06(5)	4.00(5)		3.99(5)

[a] T = 298.2 ± 0.1 K; I = 0.10 ± 0.01 M in KNO_3. The protonation constants of A and the stability constants of A with copper(II) were determined in the same experimental conditions and were compiled in Tables S3 and S4 in the Supporting Information. [b] A^{2-} indicates in general the dicarboxylate anion. [c] Values in parentheses are standard deviations in the last significant figures. [d] Determined by competition experiments by spectrophotometry in the UV region.

thus avoiding precipitation of the complexes. However, because the association constants are higher than 5 log units, the values could only be determined using data obtained by competition experiments as described in the Experimental Section (see Figures S3 and S4 in the Supporting Information). The values obtained for the equilibrium reaction $[Cu_2L]^{4+} + A^{2-} \rightleftharpoons [Cu_2L(A)]^{2+}$ are 7.70(6), 8.57(5), and 9.79(1) log units for A = ph^{2-}, iph^{2-}, and tph^{2-}, respectively.

Remarkably high association constants in the range of 7.34–10.01 log units were determined for the binding of $[Cu_2L]^{4+}$ to the dianionic form of the substrates, and, in fact, to the best of our knowledge, these are the highest association constant values reported for the binding of dicarboxylates in aqueous solution. In all cases the association constants are much larger than the determined values of the coordination of the monocarboxylate anions acetate (ac^{-}) and benzoate (bz^{-}) to $[Cu_2L]^{4+}$, which are 4.09 and 5.10 log units, respectively (see Table S5 in the Supporting Information), suggesting that all dicarboxylate anions studied in this work are coordinated in a bridging mode.

A very well defined peak of selectivity was found for the series of aliphatic dicarboxylates, as shown in Figure 2. The effective binding increases with the chain length reaching a maximum for adi^{2-}, the substrate with the chain of four carbon atoms between the carboxylate groups, after which they drop again for the longer pim^{2-}. In the aromatic dicarboxylate series the best fit was found for tph^{2-}, which, as with adi^{2-}, has four carbon atoms between the carboxylate groups. However, the receptor is unable to distinguish aliphatic from aromatic dicarboxylates of about the same size as the selectivity is based mainly in the length that separates the two carboxylate moieties. Nonetheless, as shown in the competition diagram[9] represented in Figure 3, at pH 7.2 adi^{2-} is clearly the preferred anion by the copper cryptate receptor with the

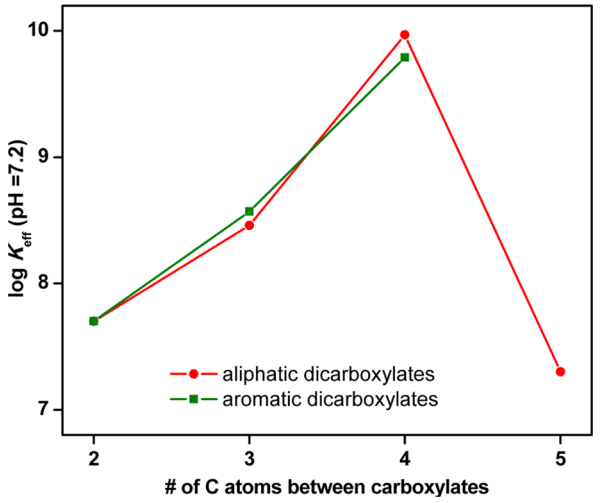

Figure 2. Representation of log K_{eff} at pH = 7.2 as a function of the number of carbon atoms linking the two carboxylate groups of the substrates. $K_{eff} = \Sigma[RH_{i+j}A]/\Sigma[H_iA]\Sigma[H_jR]$, where R is the receptor $[Cu_2L]^{4+}$ and A is the anionic substrate.[8]

$\Sigma[Cu_2H_hL(adi)]^{(2+h)+}$ complex representing 83% of the total $\Sigma[Cu_2H_hL(A)]^{(2+h)+}$ species.

Curiously, although suc^{2-} and ph^{2-} were expected not to have length enough to be able to bridge the two copper(II) centers, however the association constants for the formation of the $[Cu_2L(suc)]^{2+}$ and $[Cu_2L(ph)]^{2+}$ supermolecules are rather high, 7.75 and 7.70 log units, respectively. In fact these values are much larger than the corresponding values for the coordination of ac^{-} and bz^{-} to $[Cu_2L]^{4+}$ (4.09 and 5.10 log units, respectively; see Table S5 in the Supporting Information). This suggests that the cryptate is quite flexible, probably due to the methylene group of the biphenylmethane spacers,

dx.doi.org/10.1021/ic502230q | Inorg. Chem. 2015, 54, 229–240

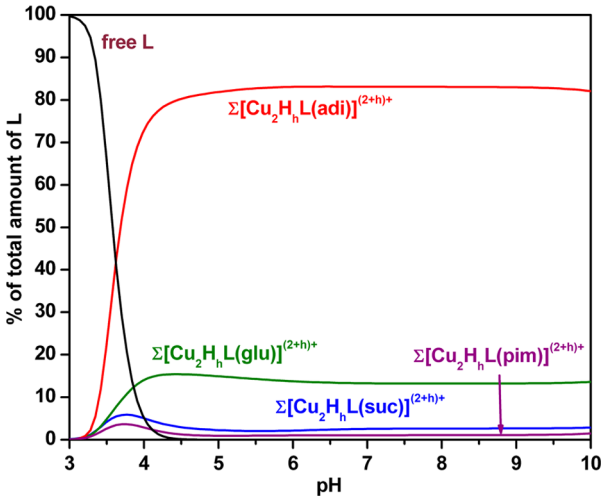

Figure 3. Distribution diagram of the overall amounts of supramolecular species formed between $[Cu_2H_hL]^{(2+h)+}$ and each dicarboxylate anion. $C_{Cu} = 2C_L = 2C_A = 2.0 \times 10^{-3}$ M.

and it is able to adjust to the length of the substrate, although with the corresponding energetic penalty.

For a 1:1:1 Cu^{2+}:L:A^{2-} ratio its is also possible to form associated entities of the type $[CuH_nL(A)]^{n+}$ by reaction of monuclear copper(II) complexes with the dicarboxylate HA^- or A^{2-} forms (see Table 2). These species result from the coordination of one of the carboxylate units to the copper center and the possible interaction of the other carboxylate group with the protonated amine groups of the other head of the cryptand, through electrostatic and hydrogen bonding interactions. However, it is necessary to emphasize that at 2:1:1 Cu^{2+}:L:A^{2-} ratio the entities involving mononuclear copper(II) complexes are not significant due to the very high stability of the $[Cu_2H_hL(A)]^{(2+h)+}$ species (see as an example the distribution diagrams presented in Figure S5 in the Supporting Information).

Spectroscopic Studies. In order to get further insight on the binding event and on the characteristics of the copper binding site the vis absorption and electron paramagnetic resonance (EPR) spectra of $[Cu_2L]^{4+}$ and $[Cu_2L(A)]^{2+}$ (Figure 4) were recorded at pH 7.2.

The absorption spectrum of $[Cu_2L]^{4+}$ at pH 7.2 (Figure 4) showed a maximum at 840 nm and a shoulder at 700 nm indicative of trigonal-bipyramidal geometry,[10] as observed in other copper complexes of tren [tris(2-aminoethyl)amine] and other tren-derived compounds found in the literature.[10−12] The corresponding EPR spectrum could only be simulated (Figure S6 in the Supporting Information) by considering two isolated copper(II) sites, with slightly different values of g and hyperfine splitting (Supporting Information Table S6). However, both copper(II) sites have three different principal values of g, with $(g_1 + g_2)/2 > g_3$ and $g_3 < 2.04$, and hyperfine splitting values in agreement with distorted trigonal bipyramidal geometries.[13]

The absorption spectra of $[CuN_4O(suc)]^{2+}$, $[CuN_4O(glu)]^{2+}$, and $[CuN_4O(adi)]^{2+}$ on the other hand showed two equally intense bands, which is consistent with a square-pyramidal distorted trigonal bipyramidal CuN_4O chromophore.[14−16] The EPR spectrum of $[Cu_2L(adi)]^{2+}$ in particular could be simulated considering two isolated copper centers (Figure S7 in the Supporting Information), yielding a set of g values for which the calculated parameter R[17] [$R = (g_2 - g_3)/(g_1 - g_2)$ with $g_1 > g_2 > g_3$] assumes a value of ≈1 (Supporting Information Table S6), typical of a square-pyramidal distorted trigonal bipyramidal geometry.[14]

On the other hand, the EPR spectra of $[Cu_2L(suc)]^{2+}$ and $[Cu_2L(glu)]^{2+}$ do not show the usual four-line hyperfine signal typical of mononuclear copper(II) complexes but instead a splitting that is indicative of exchange interaction between two copper(II) atoms and suggests that suc^{2-} and glu^{2-} are bound in a bridging mode.

In the case of the absorption spectrum of $[Cu_2L(pim)]^{2+}$ at pH = 7.2 (Figure 4) the higher energy band becomes more intense than the lower energy one, indicating that the geometry is closer to a square-pyramidal geometry.[10] Accordingly, g values obtained by simulation of the corresponding EPR spectrum (Figure S8 in the Supporting Information), by considering two slightly different isolated copper(II) sites, yielded R parameters of 1.4 and 0.2. This means that one copper center is in a square-pyramidal distorted trigonal

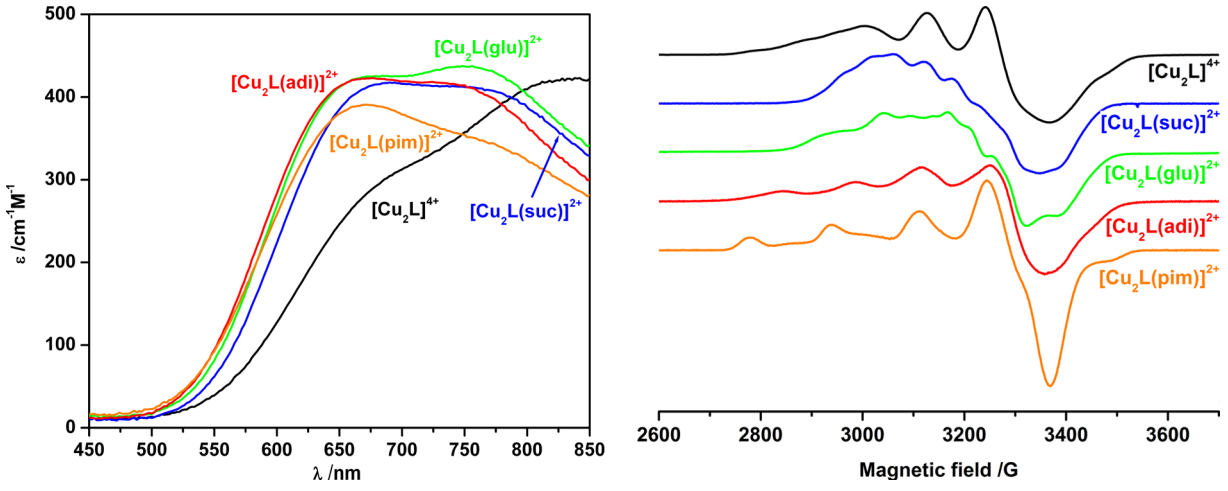

Figure 4. Vis absorption and X-band EPR spectra of $[Cu_2L]^{4+}$ and its associations with the aliphatic dicarboxylates. The complexes were prepared at 1.0×10^{-3} M and pH = 7.2 in H_2O/MeOH (1:1 (v/v)) for the spectrophotometric and at 5.0×10^{-4} M in H_2O/MeOH/DMSO solutions (1:1:2 (v/v)) for the EPR measurements. The EPR spectra were recorded at a microwave power of 2.0 mW, frequency (ν) of 9.67 GHz, and T = 89 K.

dx.doi.org/10.1021/ic502230q | Inorg. Chem. 2015, 54, 229−240

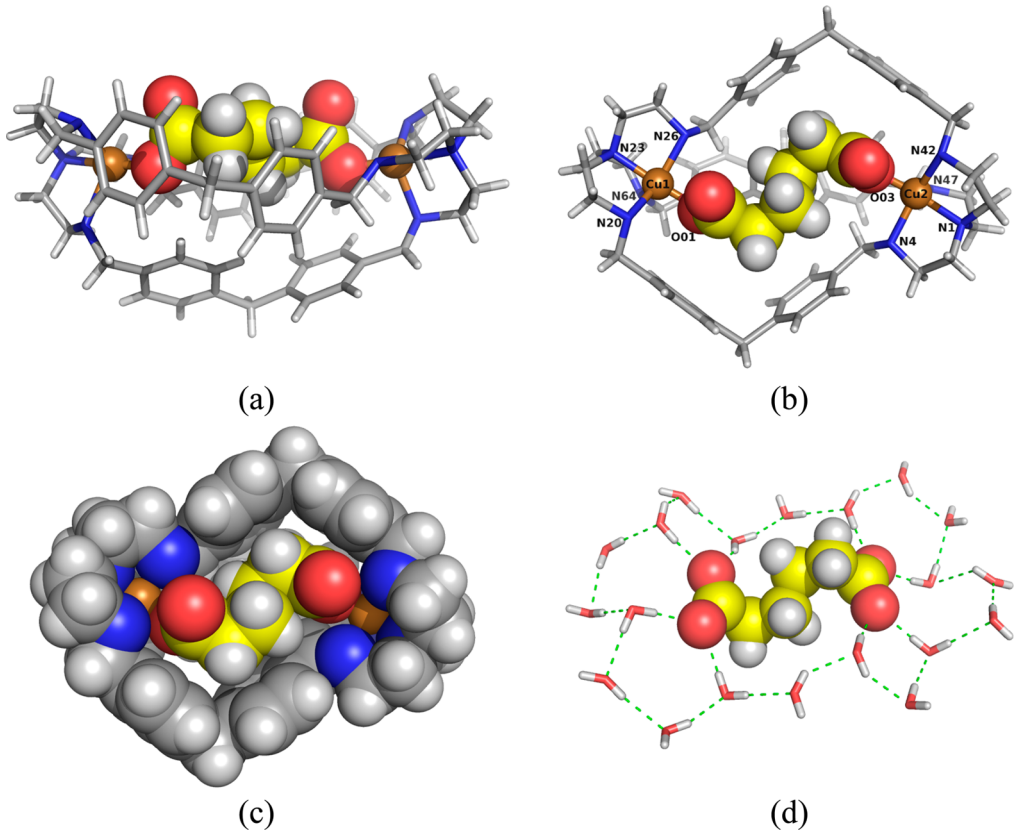

Figure 5. X-ray crystal structure of the $[Cu_2L(\mu\text{-adi})]^{2+}$ complex cation showing different structural features: (a) the side view; (b) top view; (c) top view represented in space filling model emphasizing the perfect fit within the bowl-shaped cavity; (d) X-ray structure of $adi^{2-}\cdot 20H_2O$ assuming a gauche−anti-gauche conformation.[19]

bipyramidal geometry (R = 1.4) while the other is in a square-pyramidal geometry (R = 0.2).

With regard to the aromatic substrates (Supporting Information Figure S9), the vis spectrum of $[Cu_2L(tph)]^{2+}$ also presents two equally intense bands at 680 and 770 nm consistent with the square-pyramidal distorted trigonal bipyramidal geometry. However, the vis and EPR spectra of $[Cu_2L(ph)]^{2+}$ and $[Cu_2L(iph)]^{2+}$ are characteristic of trigonal-bipyramidal geometries (see Figure S9 and Table S6 in the Supporting Information).

The spectroscopic studies suggest that the binding and encapsulation of the dicarboxylate anions by the $[Cu_2L]^{4+}$ receptor is accompanied by a rearrangement of the conformation of the copper(II) cryptate such that a distortion from trigonal-bipyramidal to square-pyramidal geometry of the copper site occurs. This distortion requires an increase of one of the $N_{eq}-Cu-N_{eq}$ angles of the trigonal planes and is expected to cause an opening of the entrance of the cavity of the cryptate.[18] The long size of the pim^{2-} substrate appears to require further opening of the entrance of the cavity; thus, the larger $N_{eq}-Cu-N_{eq}$ is further increased leading to a geometry that is closer to a square-pyramidal one.

Single-Crystal X-ray Diffraction Studies. The molecular structure of $[Cu_2L(\mu\text{-adi})](NO_3)_2\cdot 10.8H_2O$ is shown in Figure 5 along with the relevant atomic notation adopted. Selected bond lengths and angles are given in Table 3.

The cryptand adopts a bowl conformation in which the adi^{2-} anion is perfectly nested between the two copper(II) centers, located at 9.645(9) Å from one another. Each copper center is pentacoordinate and bound to four nitrogen atoms of a tren subunit of L and to an oxygen atom of the encapsulated anion. The trigonal distortion calculated using the index structural parameter τ (τ = 0 for a perfect square-pyramidal geometry and τ = 1 for an ideal trigonal-bipyramidal geometry)[18] assumes values of 0.67 and 0.57 for Cu(1) and Cu(2), respectively, which is consistent with square-pyramidal distorted trigonal bipyramidal stereochemistries. Indeed, within the trigonal planes the $N_{eq}-Cu-N_{eq}$ angles deviate considerably from 120°: 135.9(3)°, 112.6(3)°, and 108.5(3)° in Cu(1) and 139.6(3)°, 112.7(4)°, and 105.7(4)° in Cu(2), which implies a significant distortion from a regular trigonal bipyramid. In addition, in both centers the larger $N_{eq}-Cu-N_{eq}$ angle lies opposite to the longest in-plane Cu−N distance [2.233(6) Å for Cu(1)−N(64) and 2.177(1) Å for Cu(2)−N(47)], a typical feature of square-pyramidal distorted trigonal bipyramidal stereochemistry.[14−16] This is in perfect agreement with the information obtained from the respective absorption spectrum in solution (Figure 4).

The adi^{2-} anion is encapsulated and bound in a monodentate η^1 mode with Cu(1)−O(01) and Cu(2)−O(03) distances of 1.901(5) and 2.062(6) Å, respectively. The dianion assumes a gauche−anti-gauche conformation with torsion angles of 55.6(1)°, 168.8(9)°, and −65.0(9)° and the coordinated carboxylate oxygen atoms at a distance of 6.504(9) Å. It is curious to establish the parallel of these data with those of the crystal structure of a water−adi^{2-} cluster sandwiched between two layers of a silver(I) polymer complex (Figure 5d).[19] In this case the adi^{2-} anion is surrounded by a 20-membered water ring assuming a gauche−anti-gauche conformation with torsion angles of 67.7°, 173.7°, and −65.4° and the carboxylate oxygen

dx.doi.org/10.1021/ic502230q | Inorg. Chem. 2015, 54, 229−240

Table 3. Selected Bond Distances (Å) and Angles (deg) in the Coordination Spheres of the $[Cu_2L(\mu\text{-adi})]^{2+}$ and $[Cu_2L(\mu\text{-tph})]^{2+}$ Cation Complexes

complex	$[Cu_2L(\mu\text{-adi})]^{2+}$	$[Cu_2L(\mu\text{-tph})]^{2+}$
	Bond Lengths/Å	
Cu1−O01	1.901(5)	1.938(7)
Cu1−N20	2.062(6)	2.083(8)
Cu1−N23	2.016(8)	2.042(9)
Cu1−N26	2.101(7)	2.118(7)
Cu1−N64	2.233(6)	2.180(7)
Cu2−O03	1.928(6)	1.922(6)
Cu2−N1	2.033(1)	2.043(9)
Cu2−N4	2.087(6)	2.107(7)
Cu2−N42	2.073(8)	2.109(8)
Cu2−N47	2.177(1)	2.197(7)
	Bond Angles/deg	
N23−Cu1−O01	175.8(3)	178.2(3)
N23−Cu1−N20	85.1(3)	84.7(3)
N23−Cu1−N26	85.1(3)	85.2(3)
N23−Cu1−N64	82.3(3)	84.3(3)
O01−Cu1−N20	96.1(2)	93.9(3)
O01−Cu1−N26	91.3(2)	94.9(3)
O01−Cu1−N64	101.1(2)	97.2(3)
N20−Cu1−N26	135.9(3)	132.1(3)
N20−Cu1−N64	108.5(3)	108.3(3)
N26−Cu1−N64	112.6(3)	117.2(3)
N1−Cu2−O03	173.8(3)	175.9(3)
N1−Cu2−N4	83.6(3)	85.3(3)
N1−Cu2−N42	88.2(4)	84.8(3)
N1−Cu2−N47	84.1(5)	84.6(3)
O03−Cu2−N4	91.0(3)	94.6(3)
O03−Cu2−N42	94.0(3)	92.4(3)
O03−Cu2−N47	100.3(5)	99.1(3)
N4−Cu2−N42	139.6(3)	133.9(3)
N4−Cu2−N47	105.7(4)	116.2(3)
N42−Cu2−N47	112.7(4)	107.5(3)

atoms at a distance of 6.33 Å, values quite similar to those found in the crystal structure of $[Cu_2L(\mu\text{-adi})]^{2+}$. It should be noticed that it was previously demonstrated by photoelectron spectroscopy in combination with molecular dynamics simulations that although in the gas phase the adi^{2-} dianion assumes a linear geometry due to the electrostatic repulsion of the two carboxylate groups, in aqueous environment the conformation changes to a folded conformation.[20] Therefore, the structure of the cryptand in $[Cu_2L]^{4+}$ has enough flexibility to be capable of adapting to the more stable structure of the dianion, which is the gauche−anti-gauche conformation found in solution. Indeed, unlike what happen in all tren-derived copper(II) cryptates,[6] the N(23)−Cu(1)−O(01) and N(1)−Cu(2)−O(03) axis are not collinear as a consequence of the "zigzag" conformation adopted by the studied cryptand (see Figure 5b,c), which is complementary to that of the encapsulated adi^{2-} anion.

The encapsulation of the adi^{2-} anion is clearly favored by two intramolecular C−H···π interactions (3.527(10) and 3.538(13) Å) that induce a better fitting of the adipate within the cage. Another C−H···π interaction is observed within the cage (3.610(8) Å), reinforcing its bowl shape. Furthermore, there are several short-ring interactions as well as a few C−H···π contacts that are responsible for the dense packing observed in these structures (Tables S7 and S8 in the Supporting Information).

The bowl shape of the cryptand leaves the dianion only partially exposed to water molecules, resulting in the almost complete desolvation of the substrate which must give an important contribution to the overall stability of the complex. Only three water molecules interact with the encapsulated dianion (see Figure S12 in the Supporting Information): two water molecules bridge the two carboxylate moieties of the same anion (O···Ow···Ow···O, 2.78(3), 2.86(3), and 2.76(2) Å) and a third water molecule bridges the anion with a secondary amine from the cryptand (O···Ow···N, 2.64(2) and 3.041(3) Å).

The molecular structure of $[Cu_2L(\mu\text{-tph})](ClO_4)_2\cdot MeOH\cdot 4H_2O$ is shown in Figure 6 along with the relevant atomic notation adopted. Selected bond lengths and angles are given in Table 3. The conformation adopted by the cryptand in the $[Cu_2L(\mu\text{-tph})]^{2+}$ cascade complex is rather different from the zigzag one observed in $[Cu_2L(\mu\text{-adi})]^{2+}$, although the tph^{2-} is also nested between the two copper(II) centers. In the $[Cu_2L(\mu\text{-tph})]^{2+}$ cascade complex cation the metal ions are separated by a much longer distance of 10.803(14) Å, which indicates that the cryptand architecture is rather flexible. As before, each copper center is pentacoordinate and bound to four nitrogen atoms of a tren subunit of L and to an oxygen atom of the encapsulated dianion. The index structural parameter τ assumes values of 0.78 and 0.69 for Cu(1) and Cu(2), respectively, which is also consistent with square-pyramidal distorted trigonal bipyramidal stereochemistries, but with a smaller distortion from a regular trigonal bipyramid than in $[Cu_2L(\mu\text{-adi})](NO_3)_2\cdot 10.8H_2O$. Accordingly, within the trigonal planes the $N_{eq}-Cu-N_{eq}$ angles deviate less from 120°: 132.1(3)°, 117.2(3)°, and 108.3(3)° in Cu(1) and 133.9(3)°, 116.2(3)°, and 107.5(3)° in Cu(2). Again, the coordination geometry adopted by the copper centers in the crystal structure is the same as that found in solution.

The tph^{2-} anion is encapsulated and bound in a monodentate η^1 mode with Cu(1)−O(01) and Cu(2)−O(03) distances of 1.938(7) and 1.922(6) Å, respectively, and the coordinated carboxylate oxygen atoms are at a distance of 6.946(11) Å. This encapsulation is favored by several long $\pi\cdots\pi$ interactions between the tph^{2-} anion and the surrounding rings in the cage (Cg···Cg, 4.793(7), 4.549(6), 4.566(5), 5.358(5), 4.548(6), 4.961(6), and 5.477(6) Å; Table S9 in the Supporting Information). In spite of the structural differences between both structures, the bite length (the distance between the two coordinated carboxylate oxygen atoms) is not very different from that found in $[Cu_2L(\mu\text{-adi})](NO_3)_2\cdot 10.8H_2O$ [6.504(9) Å]. Also noteworthy is the fact that in this case the N(23)−Cu(1)−O(01) and N(1)−Cu(2)−O(03) axes are practically collinear, as a consequence of the extended conformation adopted by the cryptand (see Figure 6c.), which leaves the copper(II) centers at a longer distance from each other. Water molecules interact with the complex via O02···O2M···O2w···N20 (2.722(9), 2.996 (8), and 2.990(9) Å) and with the perchlorate via a O3P···O3W (3.019(9) Å) long hydrogen bond. The supramolecular arrangement of the cryptand molecules showed the formation of alternated layers of $[Cu_2L(\mu\text{-tph})]$ and water···methanol···nitrate clusters in the *ac* plane (Figure S13).

Hirshfeld Surface Analysis. The interactions of the anionic substrates with its surroundings is possible to study by using Hirshfeld surface analysis,[21] generated from

dx.doi.org/10.1021/ic502230q | Inorg. Chem. 2015, 54, 229−240

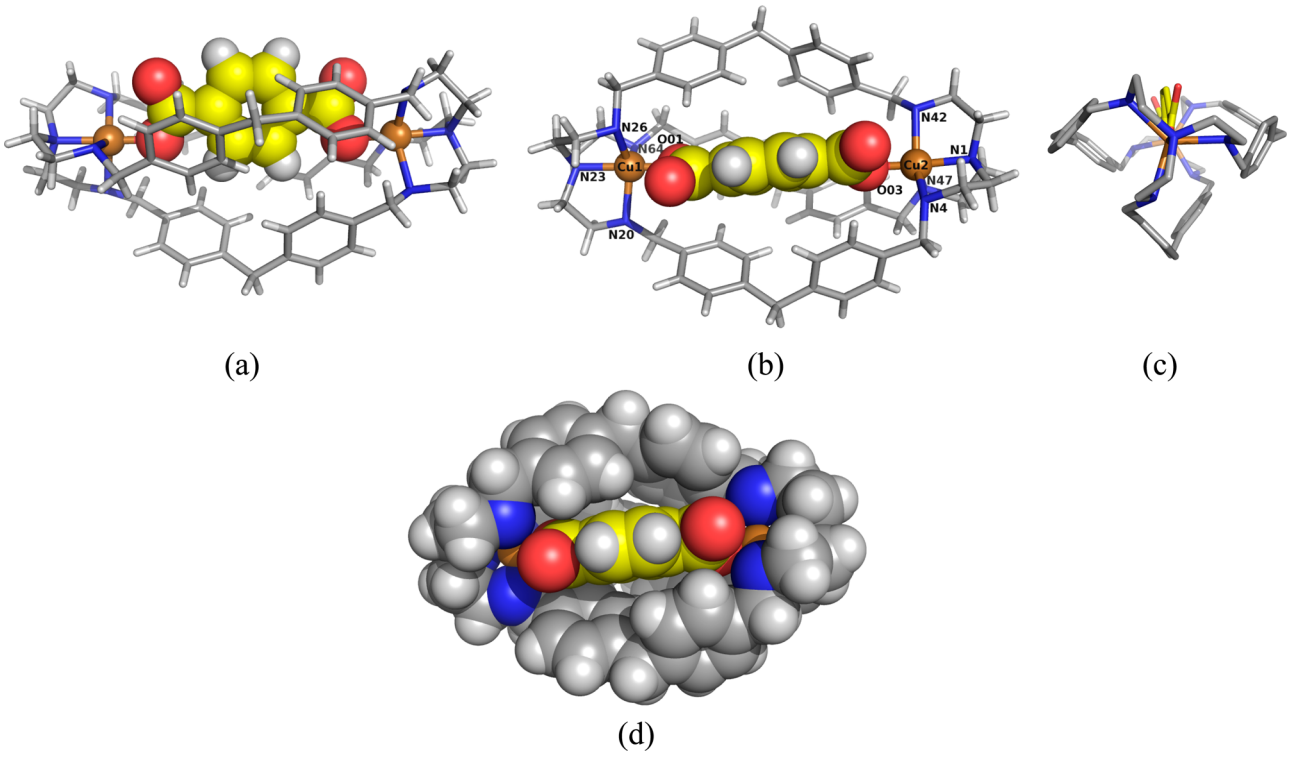

Figure 6. X-ray crystal structure of the $[Cu_2L(\mu\text{-tph})]^{2+}$ complex cation showing different structural features: (a) the side view; (b) top view; (c) view along the bridgehead N,N axis; (d) top view represented in the space filling model emphasizing the perfect fit within the bowl-shaped cavity.

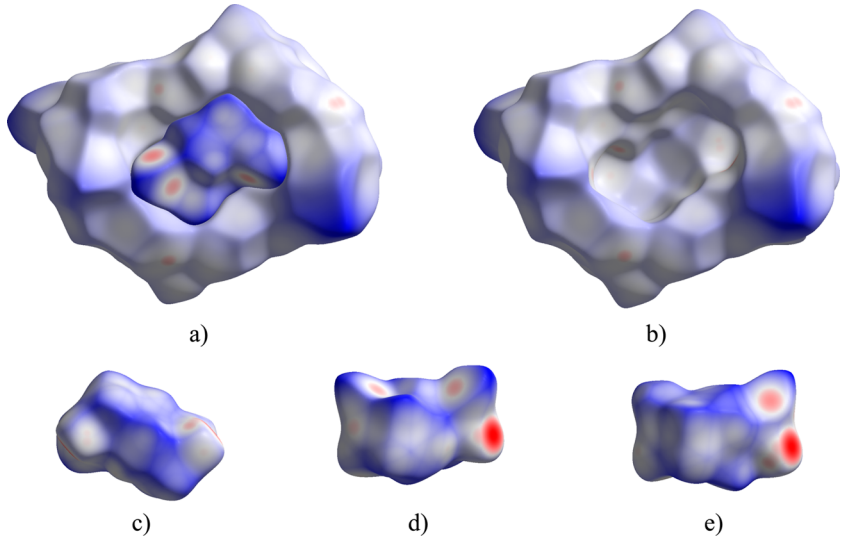

Figure 7. Hirshfeld surfaces of $[Cu_2L(\mu\text{-adi})]^{2+}$ mapped with d_{norm}: (a) view emphasizing the perfect fit of adi^{2-} inside the cavity of the cryptate; (b) view of the cavity of the cryptate; (c–e) bottom and side views of Hirshfeld surface of adi^{2-} anion.

CrystalExplorer 3.1.[22] The program can calculate the distances from the Hirshfeld surface to the nearest atoms outside (d_e) and the distances from these to the inside of the surface (d_i). These distances mapped on the Hirshfeld surface allow the visualization of all intermolecular close contacts in a crystal. Plots of d_e vs d_i give rise to two-dimensional fingerprint plots that provide a quantitative summary of the nature and type of intermolecular contacts and the relative contribution of each to the Hirshfeld surface area.[23,24]

Hirshfeld surfaces mapped with $d_{norm} = [(d_i - r_i^{vdW})/r_i^{vdW}] - [(d_e - r_e^{vdW})/r_e^{vdW}]$, where r^{vdW} is the van der Waals radius of the appropriate atom internal or external to the surface, allows visualization of intermolecular interactions by displaying a surface with a red–white–blue color code, where red spots highlight shorter contacts, white regions represent contacts around the van der Waals distance, and blue areas are without contacts.[24]

The Hirshfeld surfaces of $[Cu_2L(\mu\text{-adi})]^{2+}$ mapped with d_{norm} are represented in Figure 7.

It is especially evident in Figure 7a that the adi^{2-} anion is perfectly nested inside the cavity of the cryptate, being only partially exposed to outside water molecules (the three red spots in the top surface of adi^{2-} correspond to the three hydrogen bonds between water molecules and the carboxylate

dx.doi.org/10.1021/ic502230q | Inorg. Chem. 2015, 54, 229–240

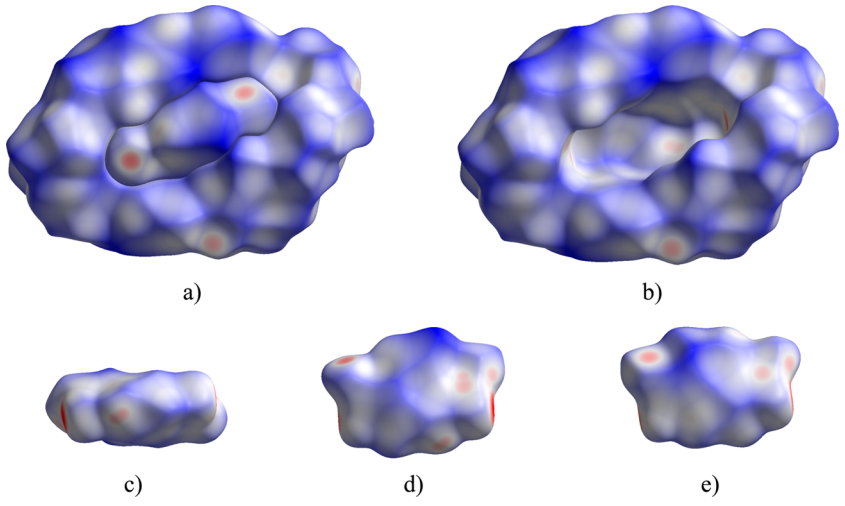

Figure 8. Hirshfeld surfaces of $[Cu_2L(\mu\text{-tph})]^{2+}$ mapped with d_{norm}: (a) view emphasizing the perfect fit of tph^{2-} inside the cavity of the cryptate; (b) view of the cavity of the cryptate; (c–e) bottom and side views of Hirshfeld surface of tph^{2-}.

oxygen atoms). It is worth noting that the inside of the cavity is mainly of white color and that the surface of the anion has also many white regions. This means that in all of these regions the contacts are around the van der Waals distance and that this type of interaction contributes to the overall stability of the supermolecule. Analysis of the fingerprint plot of the Hirshfeld surface of adi^{2-} (see Figure S14 in the Supporting Information) showed that H···H and H···C contacts make up 44.7% of the Hirshfeld surface area of adi^{2-}.

The Hirshfeld surfaces of $[Cu_2L(\mu\text{-tph})]^{2+}$ mapped with d_{norm} (Figure 8) also highlight the perfect fit of tph^{2-} inside the cavity of $[Cu_2L]^{4+}$ (Figure 8a). The shape of the cavity (Figure 8b) is clearly different from that of $[Cu_2L(\mu\text{-adi})]^{2+}$ which shows the conformational adaptability of the cryptate. Also in this case both the surface of the inside of the cavity and the surface of the anion are mainly colored white, evidencing the existence of several contacts around the van der Waals distance. It is also noticeable a faint-red spot in the "bottom" of the surface of tph^{2-} (Figure 8c) which corresponds to a C–H···π interaction. Analysis of the fingerprint plot of the Hirshfeld surface of tph^{2-} (see Figure S15 in the Supporting Information) shows that H···H (25.2%), C···H (15.3%), H···C (7.6%), and C···C (6.6%) contacts correspond to 54.7% of the Hirshfeld surface area of tph^{2-}.

The Hirshfeld surface analysis of both cascade complexes allowed one to conclude that the receptor adapts its conformation to accommodate these substrates in its cavity in such a way that the amount of contact area between the substrates and the walls of the receptor is maximized for the establishment of multiple van der Waals interactions.

CONCLUSION

In the present study was shown that the cryptand L forms rather stable dinuclear copper(II) complexes, with the $[Cu_2L]^{4+}$ species reaching its maximum percentage at pH 6.6, at which all studied dicarboxylates are mainly in the dianionic form.

The cryptate binds the dicarboxylate substrates with remarkably high association constants in the range of 7.34–10.01 log units. Indeed these are, to the best of our knowledge, the highest association constant values reported for the binding of dicarboxylate anions in aqueous solution. The association constants are in fact high for every dicarboxylate substrate studied, which suggests that all of them are bound in a bridging mode. This indicates that the cryptand of the copper(II) complex is quite flexible, probably due to the methylene group of the biphenylmethane spacers, and is able to adjust to the size and form of the substrate. Additionally, the copper(II) complexes have enough "plasticity" allowing it to adopt stereochemistries varying over an appreciable range of distortion within a given coordination number.

A very well defined peak of selectivity was found for the binding affinity of the dicopper(II) complex of L with the studied series of dianions, with the association constant values increasing with the chain length and reaching the maximum for substrates with four carbon atoms separating the carboxylate groups (adi^{2-} and tph^{2-} anions).

The spectroscopic studies showed that the binding and encapsulation of the dicarboxylates by the cryptate causes a distortion from trigonal-bipyramidal to square-pyramidal geometry of the copper sites, consistent with an opening of the entrance of the cavity of the cryptate. Single-crystal X-ray diffraction studies of the adi^{2-} and tph^{2-} cascade complex structures were in agreement with the solution studies, showing that indeed the receptor is able to adjust its conformation to the structural requirements of the substrate. The crystal structures confirmed that the copper(II) centers adopt square-pyramidal distorted trigonal bipyramidal stereochemistries, causing the cryptate to adopt a bowl-shaped conformation in which the substrate is perfectly nested between the two copper centers. For the two best bound substrates, adi^{2-} and tph^{2-}, similar distances between the coordinated carboxylate oxygen atoms were found. This leads to the conclusion that the observed selectivity arises from the fact that these substrates have the appropriate bite length. However, it is clear from the Hirshfeld surface analyses of both cascade complexes that the establishment of van der Waals and C–H···π interactions between the substrates and the walls of the receptor also contributes to the stability of the associations and to the observed selectivity.

EXPERIMENTAL SECTION

General Considerations. All solvents and reagents used were commercially purchased reagent grade quality and used as supplied without further purification, except 4,4′-methylenedibenzaldehyde which was prepared according to literature

dx.doi.org/10.1021/ic502230q | Inorg. Chem. 2015, 54, 229–240

methods.[25] NMR spectra used for characterization of products were recorded on a Bruker Avance 400 instrument. The reference used for the ^{1}H NMR measurements in $CDCl_3$ was tetramethylsilane (TMS) and in D_2O the 3-(trimethylsilyl)-propanoic acid-d_4 sodium salt. Peak assignments are based on peak integration and multiplicity for one-dimensional (1D) ^{1}H spectra and on COSY, NOESY, and HMQC experiments (Figures S16−S20 in the Supporting Information). Microanalyses were carried out by the ITQB Microanalytical Service. The electronic spectra were recorded with a UNICAM UV−vis spectrophotometer model UV-4.

Caution! *Although no problems were encountered during this work with the perchlorate salts, these compounds should be considered potentially explosive.*

Syntheses. *L·6HNO$_3$.* The cryptand L was synthesized with a slightly improved yield by a modification of the literature procedure.[7] 4,4′-Methylenedibenzaldehyde (1758 mg, 7.84 mmol) was quickly added to a magnetically stirred solution of tren (764 mg, 5.23 mmol) in 2:1 DCM/MeOH (300 mL). The mixture was left under stirring during the night. The DCM was removed by evaporation, and methanol was added (100 mL). Then, solid $NaBH_4$ (5.9 g, 156.8 mmol) was added in small portions to the mixture. After the addition was completed, the mixture was left under stirring at room temperature (rt) for 2 h and under reflux for 4 h. The solution was evaporated under vacuum almost to dryness, then water was added, and the entire methanol was evaporated. The solution was made strongly basic with 6 M KOH and extracted with $CHCl_3$ (3 × 50 mL). The organic portions were collected in an Erlenmeyer flask, dried over anhydrous sodium sulfate, filtered, and evaporated to dryness. The compound was dissolved in MeOH (200 mL), and concentrated HNO_3 (0.9 mL) was added. The mixture was boiled and allowed to slowly reach rt. A white precipitate formed which was filtered and washed with cold MeOH to yield pure L·6HNO$_3$ (1857 mg, 57%). ^{1}H NMR (D_2O, 400 MHz; ppm): δ_H 7.30 (24 H, s, H−Ar), 4.04 (12 H, s, BzCH_2N), 3.99 (6 H, s, BzCH_2Bz), 2.97 (12 H; t, J = 5.0 Hz, NCH$_2$CH_2NH), 2.69 (12 H, t, J = 5.0 Hz, NCH_2CH$_2$NH). ^{13}C NMR (D_2O, 100 MHz; ppm): δ_C = 143.4 (C4, Bz) 130.9 (C2, C6, Bz), 130.4 (C3, C5, Bz), 128.8 (C1, Bz), 51.2 (CH$_2$Bz), 50.2 (NHCH$_2$CH$_2$N), 44.3 (NHCH$_2$CH$_2$N), 41.0 (BzCH$_2$Bz); Anal. Calcd for $C_{57}H_{78}N_{14}$·6HNO$_3$·0.5MeOH: C, 54.67%; H, 6.38%, N, 15.52%. Found: C, 55.00%; H, 6.72%; N, 15.24%.

Crystals of [Cu$_2$L(μ-adi)](NO$_3$)$_2$·10.8H$_2$O. To the MeOH solution (200 μL) of the cryptand L (2.0 mg, 2.3 μmol) and 91 μL of a 0.0506 M aqueous solution of $Cu(NO_3)_2$ was added hot MeOH until the precipitate dissolved. A 0.01 M solution of potassium adipate (460 μL) was then added, and the mixture was allowed to slowly cool to rt. Blue single crystals suitable for X-ray crystallographic determination were obtained within 2 days.

Crystals of [Cu$_2$L(μ-tph)](ClO$_4$)$_2$·MeOH·4H$_2$O. To the MeOH solution (200 μL) of the cryptand L (2.0 mg, 2.3 μmol) and 82 μL of a 0.056 M aqueous solution of $Cu(ClO_4)_2$ was added hot MeOH until the precipitate dissolved. A 0.01 M solution of potassium terephthalate (460 μL) was then added, and the solution was allowed to slowly cool to rt. Blue single crystals suitable for X-ray crystallographic determination were obtained within 2 days.

Potentiometric Measurements. *Reagents and Solutions.* All solutions were prepared in water/methanol (50:50 (v/v)) mixed solvent. A stock solution of the receptor was prepared at ca. 2.0 × 10^{-3} M. Stock solutions of the dicarboxylic acids (analytical grade) were prepared at about 5.0 × 10^{-2} M, and the concentrations were checked by titration with standard 0.100 M KOH solutions.

A stock solution of $Cu(NO_3)_2$ (analytical grade) was prepared at about 2.5 × 10^{-2} M and the exact concentration checked by titration with K_2H_2edta (edta = ethylenediaminetetraacetic acid) following standard methods.[26] Carbonate-free solutions of the KOH titrant were prepared from a Merck ampule diluted to 500 mL of water (freshly boiled for about 2 h and allowed to cool under nitrogen) to which 500 mL of MeOH was added. These solutions were discarded every time carbonate concentration was about 0.5% of the total amount of base. The titrant solutions were standardized by Gran's method.[27]

Equipment and Working Conditions. The equipment used was described before.[28] The ionic strength of the experimental solutions was kept at 0.10 ± 0.01 M with KNO_3; the temperature was maintained at 298.2 ± 0.1 K. Atmospheric CO_2 was excluded from the titration cell during experiments by passing purified nitrogen across the top of the experimental solution.

Measurements. The [H$^+$] of the solutions was determined by the measurement of the electromotive force of the cell, $E = (E^\circ)' + Q \log [H^+] + E_j$. The term pH is defined as $-\log [H^+]$. $(E^\circ)'$, Q, E_j, and K'_w were determined by titration of a solution of known hydrogen-ion concentration at the same ionic strength, using the acid pH range of the titration. The liquid-junction potential, E_j, was found to be negligible under the experimental conditions used. The value of K'_w was determined from data obtained in the alkaline range of the titration, considering $(E^\circ)'$ and Q valid for the entire pH range and found to be equal to $10^{-13.86}$ in our experimental conditions. Before and after each set of titrations, the glass electrode was calibrated as a [H$^+$] probe by titration of 1.000 × 10^{-3} M standard HNO_3 solution with standard KOH. Every measurement was carried out with 0.040 mmol of ligand in a total volume of 40 mL. Copper complexation experiments were performed in the presence of $Cu(NO_3)_2$ in 0.5, 1.0, and 2.0 C_{Cu}:C_L ratios. The ternary systems measurements were carried out in the simultaneous presence of copper(II), cryptand L, and dicarboxylate anions in 1:1:1 C_{Cu}:C_L:C_A and 2:1:2 C_{Cu}:C_L:C_A ratios. Each titration curve consisting typically of 100 points in the 3.0−11.0 pH range, with a minimum of two replicates undertaken. All of the anions were independently titrated in the same experimental conditions, alone and in the presence of copper(II) ion and the respective equilibrium constants used in the calculations (Tables S3 and S4 in the Supporting Information). Back-titrations with standard HNO_3 solution were performed to confirm the values of the final $(E^\circ)'$ readings.

Calculation of Equilibrium Constants. Overall protonation constants, β_i^H, of the free ligands and of the studied dicarboxylates, the overall stability constants of complexes, $\beta_{M_mH_hL_l}$, and the overall association constants of the complexes of L with the dicarboxylates, $\beta_{M_mH_hL_lA_a}$, were calculated by fitting the potentiometric data obtained for all of the performed titrations in the same experimental conditions with the HYPERQUAD program.[29] The initial computations were obtained in the form of overall constants, $\beta_{H_hL} = [H_hL_l]/[H]^h[L]^l$, $\beta_{M_mH_hL_l} = [M_mH_hL_l]/[M]^m[H]^h[L]^l$ or $\beta_{M_mH_hL_lA_a} = [M_mH_hL_lA_a]/[M]^m[H]^h[L]^l[A]^a$. The errors quoted are the

dx.doi.org/10.1021/ic502230q | Inorg. Chem. 2015, 54, 229−240

Table 4. Crystallographic Data and Experimental Details for $[Cu_2L(\mu\text{-adi})](NO_3)_2\cdot 10.8H_2O$ and $[Cu_2L(\mu\text{-tph})](ClO_4)_2\cdot MeOH\cdot 4H_2O$

compound	$[Cu_2L(\mu\text{-adi})](NO_3)_2\cdot 10.8H_2O$	$[Cu_2L(\mu\text{-tph})](ClO_4)_2\cdot MeOH\cdot 4H_2O$
chem formula	$[C_{63}H_{74}Cu_2N_8O_4]_6[NO_3]_8\cdot[O]_{47}$	$[C_{65}H_{70}Cu_2N_8O_4][ClO_4]_2\cdot CO\cdot(O)_4$
fw	8054.52	1445.30
temp (K)	150(2)	150(2)
wavelength (Å)	0.71073	0.71073
cryst form, color	block, blue	block, blue
cryst size (mm)	0.20 × 0.04 × 0.02	0.12 × 0.04 × 0.02
cryst syst	trigonal	monoclinic
space group	$R\bar{3}$	$P2_1/c$
a (Å)	23.0525(11)	19.9836(19)
b (Å)	23.0525(11)	21.015(2)
c (Å)	68.656(4)	17.6125(16)
α (deg)	90.00	90.00
β (deg)	90.00	113.248(3)
γ (deg)	120.00	90
V (Å^3)	31597(3)	6795.9
Z	3	4
d (mg·cm^{-3})	1.270	1.413
μ (mm^{-1})	0.674	0.779
θ range (deg)	1.98−25.43	2.23−25.43
reflcns collected/unique	38775/12874	48502/12364
R_{int}	0.0845	0.1304
GoF	0.998	0.985
final R indices $[I > 2\sigma(I)]$	R_1 = 0.1024, wR_2 = 0.2889	R_1 = 0.1082, wR_2 = 0.2785

standard deviations of the overall constants given directly by the program for the input data, which include all of the experimental points of all titration curves. The HYSS program[30] was used to calculate the concentration of equilibrium species from the calculated constants from which distribution diagrams were plotted. The species considered in a particular model were those that could be justified by the principles of coordination and supramolecular chemistry.

Absorption and X-Band EPR Spectra. Solutions of $[Cu_2L]^{4+}$ and $[Cu_2L(A)]^{2+}$ (A being suc^{2-}, glu^{2-}, adi^{2-}, pim^{2-}, tph^{2-}, iph^{2-}, or ph^{2-}) were prepared in H_2O/MeOH (1:1 (v/v)) solution and 1.0 × 10^{-3} M concentration, and the pH was adjusted to 7.2 with small additions of either standard KOH or HNO_3 solutions. All absorption spectra were recorded from 450 to 850 nm at T = 298.2 ± 0.1 K. To these solutions dimethyl sulfoxide (DMSO) was added in a 1:1 proportion and the EPR spectra recorded at a microwave power of 2.0 mW, frequency (ν) of 9.67 GHz, and T = 89 K. EPR spectra were simulated using SpinCount software, created by Professor M. P. Hendrich at Carnegie Mellon University. SpinCount is available at http://www.chem.cmu.edu/groups/hendrich/.

UV Competition Experiments. *Reagents and Solutions.* Stock solutions of $[Cu_2L(A)]^{2+}$ (A being tph^{2-}, iph^{2-}, or ph^{2-}) were prepared in H_2O/MeOH (1:1 (v/v)) at 4.0 × 10^{-5} M by mixing a solution of $[Cu_2L](NO_3)_4$ with the potassium salt of the respective anion. The ionic strength was adjusted to 0.10 M in KNO_3, and the solutions were buffered to pH 7.2 (0.002 M HEPES). Stock solutions of the competing dicarboxylates (K_2adi or K_2suc) were prepared in H_2O/MeOH (1:1 (v/v)) at 4.0 × 10^{-4} M, and the ionic strength adjusted to 0.10 M in KNO_3 and buffered to pH 7.2 (0.002 M HEPES).

Measurements. The spectrophotometric titrations were performed in a quartz cuvette at 298.2 ± 0.1 K by adding aliquots of the stock solution competing dicarboxylate anions by means of a Hamilton syringe to 2.500 mL of stock solution of $[Cu_2L(A)]^{2+}$. After each addition the solution was kept stirring for 10 min, after which the absorption spectrum was recorded in the 250−350 nm region. Sets of 18−20 spectra were recorded for each titration. The pH value was verified before and after each titration.

Calculation of Equilibrium Constants. The molar absorbances of $[Cu_2L]^{4+}$, $[Cu_2L(tph)]^{2+}$, $[Cu_2L(iph)]^{2+}$, $[Cu_2L(ph)]^{2+}$, $[Cu_2L(adi)]^{2+}$, $[Cu_2L(suc)]^{2+}$, tph^{2-}, iph^{2-}, and ph^{2-} were measured in separate experiments and kept constant for all of the other determinations. Association constants were calculated by fitting the spectrophotometric data obtained for all the titrations with the HYPERQUAD program[29] and using as constants the K_{eff} (pH =7.2) value corresponding to the associations with of $[Cu_2L]^{4+}$ with the competing anions (adi^{2-} or suc^{2-}), previously determined by the potentiometric method. The errors quoted are the standard deviations of the overall stability constants given directly by the program for the input data, which include all of the experimental points from all titration curves.

Single-Crystal X-ray Diffraction. Crystals of $[Cu_2L(\mu\text{-adi})](NO_3)_2\cdot 10.8H_2O$ and $[Cu_2L(\mu\text{-tph})](ClO_4)_2\cdot MeOH\cdot 4H_2O$ suitable for X-ray diffraction study were mounted with Fomblin in a cryoloop. Data were collected on a Bruker AXS-KAPPA APEX II diffractometer with graphite-monochromated radiation (Mo Kα, λ = 0.17073 Å) at 150 K. The X-ray generator was operated at 50 kV and 30 mA, and the X-ray data collection was monitored by the APEX2[31] program. All data were corrected for Lorentzian, polarization, and absorption effects using SAINT[31] and SADABS[31] programs. SIR97[32] and SHELXS-97[33] were used for structure solution, and SHELXL-97 was used for full matrix least-squares refinement on F^2. These three programs are included in the package of programs WINGX-Version 1.80.05.[34] Non-hydrogen atoms were refined anisotropically. A full matrix least-squares refinement was used for the non-hydrogen atoms with anisotropic thermal

dx.doi.org/10.1021/ic502230q | Inorg. Chem. 2015, 54, 229−240

parameters. All of the hydrogen atoms were inserted in idealized positions and allowed to refine in the parent carbon atom. One of the perchlorate anions in $[Cu_2L(\mu\text{-tph})](ClO_4)_2 \cdot MeOH \cdot 4H_2O$ is disordered over two positions with a 0.6:0.4 ratio (residual density indicated that further disorder may be present in this molecule, but it was not possible to obtain a better model); a methanol molecule was located along with four water molecules, for which the hydrogen atoms were not possible to locate. In $[Cu_2L(\mu\text{-adi})](NO_3)_2 \cdot 10.8H_2O$, one of the nitrate anions is placed in a special position as well as one oxygen of a water molecule; another oxygen molecule has only a 0.5 occupancy factor; the high VOID suggests that further disordered water molecules are present in the structure, but they were not possible to model. Hydrogen atoms of the water molecules were not located from the electron density map. Molecular diagrams presented are drawn with PyMOL.[35] PLATON[36] was used to calculate bond distances and angles as well as hydrogen bond interactions. Table 4 summarizes data collection and refinement details.

CCDC-1010093 and -1010094 contain the supplementary crystallographic data for this Article. These data can be obtained free of charge from The Cambridge Crystallographic Data Centre via www.ccdc.cam.ac.uk/data_request/cif.

■ ASSOCIATED CONTENT

Supporting Information

Figures showing 1D and 2D NMR spectra of the L compound, species distribution diagrams, experimental and simulated X-band EPR spectra, X-ray crystal structure of $[Cu_2L(\mu\text{-adi})](NO_3)_2 \cdot 10.8H_2O$, Hirshfeld fingerprint plots, and COSY, HMQC, and NOESY spectra of $H_6L(NO_3)_6$, tables listing the overall and stepwise protonation constants of the L compound and of studied dicarboxylates, the overall and stepwise stability constants of the copper(II) complexes of L and of the studied dicarboxylates, X-band EPR and vis spectra data, short-ring interactions with Cg−Cg distances of the two X-ray crystal structures, additional ring interaction analysis, and a CIF document. This material is available free of charge via the Internet at http://pubs.acs.org.

■ AUTHOR INFORMATION

Corresponding Authors

*E-mail: delgado@itqb.unl.pt (R.D.).
*E-mail: pmateus@itqb.unl.pt (P.M.).

Notes

The authors declare no competing financial interest.

■ ACKNOWLEDGMENTS

We acknowledge Fundação para a Ciência e a Tecnologia (FCT) for the financial support under Project PTDC/QEQ-SUP/2718/2012. We also acknowledge support by Fundação para a Ciência e a Tecnologia (Grant RECI/BBB-BQB/0230/2012) for the NMR spectrometers as part of the National NMR Facility. The X-ray facilities thank Fundação para a Ciência e a Tecnologia for funding (Grant RECI/QEQ-QIN/0189/2012). M. C. Almeida from the ITQB Analytical Services Unit is acknowledged for providing elemental analysis and ESI-MS data. P.M. and V.A. acknowledge FCT for the fellowships SFRH/BPD/79518/2011 and SFRH/BPD/78854/2011, respectively.

■ REFERENCES

(1) (a) *Supramolecular Chemistry of Anions*; Bianchi, A., Bowman-James, K., García-España, E., Eds.; Wiley-VCH: New York, 1997. (b) Fitzmaurice, R. J.; Kyne, G. M.; Douheret, D.; Kilburn, J. D. *J. Chem. Soc., Perkin Trans.* **2002**, *1*, 841−864. (c) Gale, P. A.; Quesada, R. *Coord. Chem. Rev.* **2006**, *250*, 3219−3244. (d) Gale, P. A.; García-Garrido, S. E.; Garric, J. *Chem. Soc. Rev.* **2008**, *37*, 151−190. (e) Caltagirone, C.; Gale, P. A. *Chem. Soc. Rev.* **2009**, *38*, 520−563. (f) Gale, P. A. *Chem. Soc. Rev.* **2010**, *39*, 3746−3771.

(2) Kałużna-Czaplińska, J. *Crit. Rev. Anal. Chem.* **2011**, *41*, 114−123.

(3) Rozaini, M. Z. H. In *Atmospheric Aerosols - Regional Characteristics - Chemistry and Physics*; Abdul-Razzak, H., Ed.; InTech: Rijeka, Croatia, 2012; Chapter 11, pp 323−346.

(4) (a) Dietrich, B.; Hosseini, M. W.; Lehn, J. M.; Sessions, R. B. *J. Am. Chem. Soc.* **1981**, *103*, 1282−1283. (b) Kimura, E.; Sakonaka, A.; Yatsunami, T.; Kodama, M. *J. Am. Chem. Soc.* **1981**, *103*, 3041−3045. (c) Hosseini, M. W.; Lehn, J. M. *J. Am. Chem. Soc.* **1982**, *104*, 3525−3527. (d) Dietrich, B.; Guilhem, J.; Lehn, J. M.; Pascard, C.; Sonveaux, E. *Helv. Chim. Acta* **1984**, *67*, 91−104. (e) Hosseini, M. W.; Lehn, J. M. *Helv. Chim. Acta* **1986**, *69*, 587−603. (f) Lehn, J. M.; Meric, R.; Vigneron, J. P.; Waksman, B.; Pascard, C. *J. Chem. Soc., Chem. Commun.* **1991**, 62−64. (g) Bencini, A.; Bianchi, A.; Burguete, M. I.; García-España, E.; Luis, S. V.; Ramirez, J. A. *J. Am. Chem. Soc.* **1992**, *114*, 1919−1920. (h) Bencini, A.; Bianchi, A.; Burguete, M. I.; Dapporto, P.; Dornenech, A.; García-España, E.; Luis, S. V.; Paoli, P.; Ramirez, J. A. *J. Chem. Soc., Perkin Trans. 2* **1994**, 569−577. (i) Lu, Q.; Motekaitis, R. J.; Reibenspies, J. J.; Martell, A. E. *Inorg. Chem.* **1995**, *34*, 4958−4964. (j) Teulade-Fichou, M.-P.; Vigneron, J.-P.; Lehn, J.-M. *J. Chem. Soc., Perkin Trans. 2* **1996**, 2169−2175. (k) Paris, T.; Vigneron, J.-P.; Lehn, J.-M. *J. Inclusion Phenom. Macrocyclic Chem.* **1999**, *33*, 191−202. (l) Alfonso, I.; Dietrich, B.; Rebolledo, F.; Gotor, V.; Lehn, J.-M. *Helv. Chim. Acta* **2001**, *84*, 280−295. (m) Nelson, J.; Nieuwenhuyzen, M.; Pál, I.; Town, R. M. *Dalton Trans.* **2004**, 229−235. (n) Anda, C.; Llobet, A.; Martell, A. E.; Reibenspies, J.; Berni, E.; Solans, X. *Inorg. Chem.* **2004**, *43*, 2793−2802. (o) Miranda, C.; Escartí, F.; Lamarque, L.; Yunta, M. J. R.; Navarro, P.; García-España, E.; Jimeno, M. L. *J. Am. Chem. Soc.* **2004**, *126*, 823−833. (p) Bazzicalupi, C.; Bencini, A.; Bianchi, A.; Borsari, L.; Giorgi, C.; Valtancoli, B. *J. Org. Chem.* **2005**, *70*, 4257−4266. (q) Carvalho, S.; Delgado, R.; Fonseca, N.; Félix, V. *New J. Chem.* **2006**, *30*, 247−257. (r) Cruz, C.; Delgado, R.; Drew, M. G. B.; Félix, V. *J. Org. Chem.* **2007**, *72*, 4023−4034. (s) Arbuse, A.; Anda, C.; Martínez, M. A.; Pérez-Mirón, J.; Jaime, C.; Parella, T.; Llobet, A. *Inorg. Chem.* **2007**, *46*, 10632−10638. (t) González-Álvarez, A.; Alfonso, I.; Díaz, P.; García-España, E.; Gotor-Fernández, V.; Gotor, V. *J. Org. Chem.* **2008**, *73*, 374−382. (u) Bazzicalupi, C.; Bencini, A.; Bianchi, A.; Borri, C.; Danesi, A.; García-España, E.; Giorgi, C.; Valtancoli, B. *J. Org. Chem.* **2008**, *73*, 8286−8295. (v) Carvalho, S.; Delgado, R.; Drew, M. G. B.; Calisto, V.; Félix, V. *Tetrahedron* **2008**, *64*, 5392−5403. (x) Cruz, C.; Calisto, V.; Delgado, R.; Félix, V. *Chem.—Eur. J.* **2009**, *15*, 3277−3289. (y) Mateus, P.; Delgado, R.; Brandão, P.; Félix, V. *J. Org. Chem.* **2012**, *77*, 4611−4621.

(5) (a) Martell, A. E.; Motekaitis, R. J. *J. Am. Chem. Soc.* **1988**, *110*, 8059−8064. (b) Motekaitis, R. J.; Martell, A. E. *Inorg. Chem.* **1991**, *30*, 694−700. (c) Lu, Q.; Reibenspies, J. J.; Martell, A. E.; Motekaitis, R. J. *Inorg. Chem.* **1996**, *35*, 2630−2636. (d) Warzeska, S.; Kramer, R. *Chem. Ber.* **1995**, *128*, 115−119. (e) Bazzicalupi, C.; Bencini, A.; Bianchi, A.; Fusi, V.; García-España, E.; Giorgi, C.; Llinares, J. M.; Ramirez, J. A.; Valtancoli, B. *Inorg. Chem.* **1999**, *38*, 620−621. (f) Carvalho, S.; Cruz, C.; Delgado, R.; Drew, M. G. B.; Félix, V. *Dalton Trans.* **2003**, 4261−4270. (g) Boiocchi, M.; Bonizzoni, M.; Fabbrizzi, L.; Piovani, G.; Taglietti, A. *Angew. Chem., Int. Ed.* **2004**, *43*, 3847−3852. (h) Li, F.; Delgado, R.; Félix, V. *Eur. J. Inorg. Chem.* **2005**, 4550−4561. (i) Boiocchi, M.; Bonizzoni, M.; Moletti, A.; Pasini, D.; Taglietti, A. *New J. Chem.* **2007**, *31*, 352−356. (j) Carvalho, S.; Delgado, R.; Drew, M. G. B.; Félix, V. *Dalton Trans.* **2007**, 2431−2439. (k) Carvalho, S.; Delgado, R.; Drew, M. G. B.; Félix, V.; Figueira, M.; Henriques, R. T. *Polyhedron* **2008**, *27*, 679−687. (l) Xie, G.-Y.; Jiang, L.; Lu, T.-B. *Dalton Trans.* **2013**, *42*, 14092−14099.

(6) Mateus, P.; Lima, L. M. P.; Delgado, R. *Polyhedron* **2013**, *52*, 25−42.
(7) Jazwinski, J.; Lehn, J.-M.; Lilienbaum, D.; Ziessel, R.; Guilhem, J.; Pascard, C. *J. Chem. Soc., Chem. Commun.* **1987**, 1691−1694.
(8) Albelda, M. T.; Bernardo, M. A.; García-España, E.; Godino-Salido, M. L.; Luis, S. V.; Melo, M. J.; Pina, F.; Soriano, C. *J. Chem. Soc., Perkin Trans. 2* **1999**, 2545−2549.
(9) Bianchi, A.; García-España, E. *J. Chem. Educ.* **1999**, *76*, 1727−1732.
(10) Duggan, M.; Ray, N.; Hathaway, B.; Tomlinson, G.; Brint, P.; Pelin, K. *J. Chem. Soc., Dalton Trans.* **1980**, 1342−1199.
(11) Mateus, P.; Delgado, R.; Brandão, P.; Félix, V. *Chem.—Eur. J.* **2011**, *17*, 7020−7031.
(12) Thaler, F.; Hubbard, C. D.; Heinemann, F. W.; van Eldik, R.; Schindler, S.; Fábián, I.; Dittler-Klingemann, A. M.; Hahn, F. E.; Orvig, C. *Inorg. Chem.* **1998**, *37*, 4022−4029.
(13) Bencini, A.; Bertini, I.; Gatteschi, D.; Scozzafava, A. *Inorg. Chem.* **1978**, *17*, 3194−3197.
(14) Tyagi, S.; Hathaway, B. J. *J. Chem. Soc., Dalton Trans.* **1983**, 199−203.
(15) Harrison, W. D.; Kennedy, D. M.; Power, M.; Sheahan, R.; Hathaway, B. J. *J. Chem. Soc., Dalton Trans.* **1981**, 1556−1564.
(16) Tyagi, S.; Hathaway, B. J. *J. Chem. Soc., Dalton Trans.* **1981**, 2029−2033.
(17) Hathaway, B. J. *J. Chem. Soc., Dalton Trans.* **1972**, 1196−1199.
(18) Addison, A. W.; Rao, T. N.; Reedijk, J.; van Rijn, J.; Verschoor, G. C. *J. Chem. Soc., Dalton Trans.* **1984**, 1349−1356.
(19) Luo, G.-G.; Wu, D.-L.; Wu, J.-H.; Xia, J.-X.; Liu, L.; Dai, J.-C. *CrystEngComm* **2012**, *14*, 5377−5380.
(20) Minofar, B.; Mucha, M.; Jungwirth, P.; Yang, X.; Fu, Y.-J.; Wang, X.-B.; Wang, L.-S. *J. Am. Chem. Soc.* **2004**, *126*, 11691−11698.
(21) Spackman, M. A.; Jayatilaka, D. *CrystEngComm* **2009**, *11*, 19−32.
(22) Wolff, S. K.; Grimwood, D. J.; McKinnon, J. J.; Turner, M. J.; Jayatilaka, D.; Spackman, M. A. *CrystalExplorer* (Version 3.1); University of Western Australia: Perth, Australia, 2013; http://hirshfeldsurface.net.
(23) Spackman, M. A.; McKinnon, J. J. *CrystEngComm* **2002**, *4*, 378−392.
(24) McKinnon, J. J.; Jayatilaka, D.; Spackman, M. A. *Chem. Commun. (Cambridge, U.K.)* **2007**, 3814−3816.
(25) Peng, K.-Y.; Chen, S.-A.; Fann, W.-S. *J. Am. Chem. Soc.* **2001**, *123*, 11388−11397.
(26) Schwarzenbach, G.; Flaschka, W. *Complexometric Titrations*; Methuen: London, 1969; pp 252−258.
(27) Rossotti, F. J.; Rossotti, H. J. *J. Chem. Educ.* **1965**, *42*, 375−378.
(28) Mateus, P.; Delgado, R.; Brandão, P.; Carvalho, S.; Félix, V. *Org. Biomol. Chem.* **2009**, *7*, 4661−4673.
(29) Gans, P.; Sabatini, A.; Vacca, A. *Talanta* **1996**, *43*, 1739−1753.
(30) Alderighi, L.; Gans, P.; Ienco, A.; Peters, D.; Sabatini, A.; Vacca, A. *Coord. Chem. Rev.* **1999**, *184*, 311−318.
(31) APEX2, SAINT, and SADABS; Bruker Analytical Systems: Madison,WI, USA, 2005.
(32) Altomare, A.; Burla, M. C.; Camalli, M.; Cascarano, G. L.; Giacovazzo, C.; Guagliardi, A.; Moliterni, A. G. G.; Polidori, G.; Spagna, R. *J. Appl. Crystallogr.* **1999**, *32*, 115−119.
(33) Sheldrick, G. M. *Acta Crystallogr., Sect. A: Found. Crystallogr.* **2008**, *64*, 112−122.
(34) Farrugia, L. J. *J. Appl. Crystallogr.* **1999**, *32*, 837−838.
(35) *The PyMOL Molecular Graphics System*, Version 1.2r3pre; Schrödinger: New York; 2002.
(36) Spek, A. L. *Acta Crystallogr., Sect. D: Biol. Crytallogr.* **2009**, *65*, 148−155.

■ NOTE ADDED AFTER ASAP PUBLICATION

This paper was published on the Web on December 8, 2014, with minor text errors. The corrected version was reposted on December 9, 2014.